

## **Electronic Supplementary Information**

### **Biodetection using ZnO nanorods-based microfluidic device with a concentration gradient generator**

Yan Xie<sup>1</sup>, Yuchen Shi<sup>1</sup>, Wenhui Xie<sup>1</sup>, Mengjie Chang<sup>2</sup>, Zhenjie Zhao<sup>1,\*</sup>, Xin Li<sup>1,\*</sup>

<sup>1</sup> Engineering Research Center for Nanophotonics and Advanced Instrument, School of Physics and Electronic Science, East China Normal University, Shanghai 200062, China.

<sup>2</sup> Department of Materials Science and Engineering, Xi'an University of Science and Technology, Xi'an 710054, People's Republic of China

E-mail: xli@phy.ecnu.edu.cn (X. Li), zjzhao@phy.ecnu.edu.cn (Zhenjie Zhao)

## **1. Materials**

All the chemicals in the experiment were used without further purification. Acetone, Zinc acetate dehydrate, isopropyl (IPA), zinc nitrate hexahydrate, hexamethylenetetramine and ammonium hydroxide were purchased from Sinopharm Chemical Reagent Co., Ltd. (China). Polyethyleneimine (PEI) and Polyvinyl alcohol (PVA) were purchased from Sigma (China). Polydimethylsiloxane (PDMS, RTV-615) was purchased from Momentive (China). FITC-conjugated anti-Bovine IgG and bovine serum albumin (BSA) was purchased from ImmunoReagents, Inc (China). Human CEA antigen, human PSA antigen and FITC-conjugated anti-human CEA were all purchased from Shanghai Linc-Bio Science Co. LTD (China).

## **2. Methods**

### **2.1 Device fabrication**

To generate a stable concentration gradient, a microfluidic chip with the Christmas tree-shaped networks was fabricated using a soft lithography process. The microfluidic pattern including two inlets and five outlets was designed. Each microfluidic channel was of 200  $\mu\text{m}$  width and 50  $\mu\text{m}$  height. The master was prepared by spin-coating a layer of 50  $\mu\text{m}$  thick SU-8 photoresist (Microchem) onto a clean silicon wafer. After UV exposure and development, trimethylchlorosilane was evaporated on the mold as release agent. Then, a 10:1 mixture of base polymer to curing agent was poured onto the master and cured at 80  $^{\circ}\text{C}$  for 2 h after degassing in a vacuum. Finally, the PDMS replica were peeled off and mounted on the glass substrate with ZnO seed layer.

### **2.2 Investigation of concentration gradient**

The concentration gradient is investigated by introducing red dye through the right input at the flow rate of 0.6  $\mu\text{L}/\text{min}$  and DI water through the left input at the flow rate of 0.8  $\mu\text{L}/\text{min}$  for 10 min by a syringe pump. For further quantitative analysis of the concentration at each branch channel, the solution of Rhodamine 6G (100  $\mu\text{M}$ ) dissolved in PBS buffer was introduced into the right inlet at the flow rate of 0.6  $\mu\text{L}/\text{min}$ , and PBS buffer was introduced into the left inlet at the flow rate of 0.2  $\mu\text{L}/\text{min}$ . The final concentration in each channel was analyzed via fluorescence intensity of channels by capturing images with CCD.

### **2.2 Preparation of ZnO NR arrays**

The seed solution was obtained by the following steps: PVA (4 wt%) dissolved in DI water was stirred for 1 h at 70 °C. Then, zinc acetate dihydrate (ZAD, 1 wt%) was added into the solution and stirred for 2 h at room temperature. By spin coating the seed solution on a clean glass substrate at 3000 rpm for 1min and thermal treatment at 500 °C for 3 h, the seed layer introduced the growth of ZnO NRs was prepared. After bonding the seed layer with the microfluidic chip, ZnO NRs could be synthesized by injecting the growth solution into the microchannels at the flow rate of 20  $\mu\text{L}/\text{min}$  at 90 °C for 3 h. The growth solution contained  $\text{Zn}(\text{NO}_3)_2 \cdot 6\text{H}_2\text{O}$  (25mM), PEI (12.5mM) and HMTA (12.50 mM).

### 2.3 Fluorescence Detection

After rinsing the microchannels integrated with ZnO NR arrays with DI water for 30 min, FITC-antiIgG solution (5  $\mu\text{g}/\text{mL}$ ) were injected into one inlet at the flow rate of 0.6  $\mu\text{L}/\text{min}$  for 15 min incubation, as PBA was introduced into the other inlet at the flow rate of 0.8  $\mu\text{L}/\text{min}$ . Followed the similar procedure, CEA and PSA proteins and PBS were injected into the chip resulting in five different concentrations. The initial concentration of CEA was of 1  $\mu\text{g}/\text{mL}$  and 100 ng/mL, and the initial concentration of PSA was 100 ng/mL to reveal the detection performance. After incubation for 1 h, 5% (v / v) BSA was introduced into the outlet at the flow rate of 0.6  $\mu\text{L}/\text{min}$  for 30 min to avoid non-specific adsorption, followed by rinsing by PBS. Finally, FITC-conjugated anti-human CEA (5  $\mu\text{g}/\text{mL}$ ) was introduced into the outlet for 10 min and rinsed by PBS. Thereafter, the fluorescence intensity of all the samples was analyzed from the images captured by fluorescence microscope.

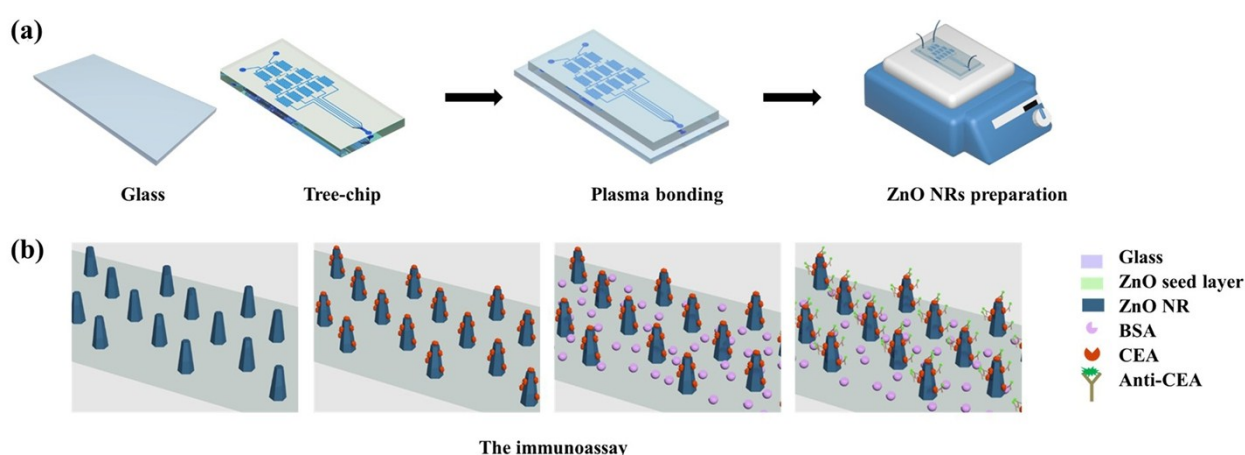


**Fig.S1** (a) Schematic of synthesis of ZnO NR arrays in microfluidic channels. (b) Schematic diagram of immunoassay in microfluidic channels integrated with ZnO NR arrays

### 3. Characterizations

Scanning electron microscopy (SEM, Hitachi, S-4800), high-resolution transmission electron microscopy (HRTEM, JEOL JEM-1400) and X-ray diffraction (XRD Rigaku, Ultima IV) were used to characterize the morphology and crystal structure of ZnO NRs. The fluorescence images were obtained by the fluorescence microscope (BDS200-FL, Optec Instrument) with CCD (Mshot 20, Micro-shot Technology Co., Ltd).

### 4. The study of concentration gradient

To optimize the biodetection condition with concentration gradient, we have investigated the effect of flow rates and the exposure time for R6G solution. As we aimed to obtain the linear concentration variation from 0 to 100 %, the concentration should be 0, 25 %, 50%, 75% and 100% of 5  $\mu\text{g}/\text{mL}$  in channel 1, 2, 3, 4 and 5. Fig. S1 shows the fluorescence images of five channels, in which the fluorescence intensity increased rapidly with the concentration from the channel 1 to the channel 5. Although the flow rates of two branches were the same as 2  $\mu\text{L}/\text{min}$  (Fig. S2a), the concentration variation is not linear, which is probably owing to the viscosity of two different solutions and the asymmetry of microfluidic channel caused during fabrication process. When increasing the flow rate of PBS, the fluorescence intensity decreased evidently in Fig. S2b-d. The quantitative analysis (Fig. S2e) showed that by increasing the flow rate of PBS with the same exposure time of 120 ms, the linear variation can be obtained. After further increased the flow rate of PBS and the exposure time (200 ms), highly sensitive concentration variation can be achieved indicating better mixing in the channels.<sup>1</sup>

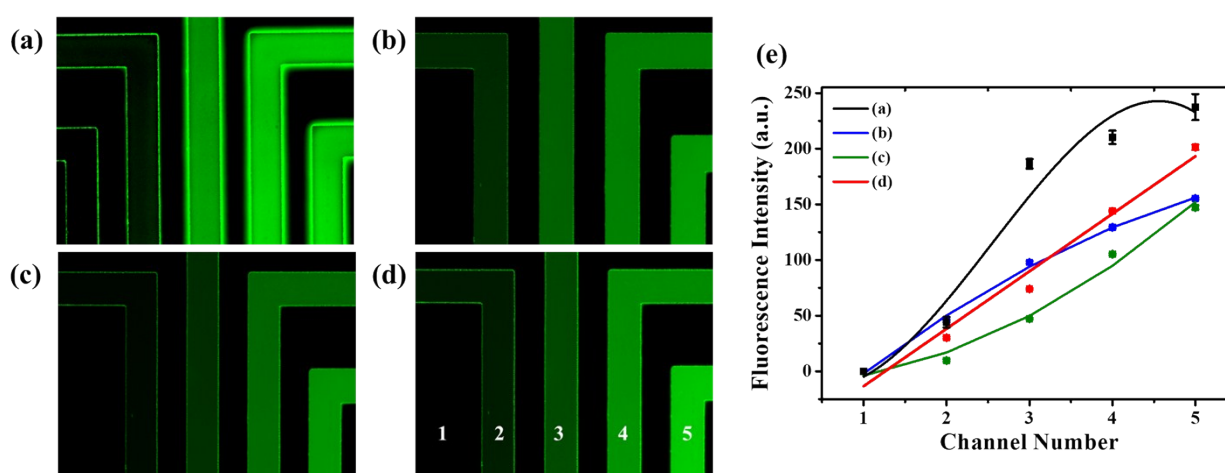


**Fig.S2** Optimization of the concentration gradient of R6G. (a) PBS and R6G were perfused into channels both at the flow rate of 2  $\mu\text{L}/\text{min}$  with exposure of 120 ms; (b) PBS and R6G were perfused at the flow rates of 0.35  $\mu\text{L}/\text{min}$  and 0.2  $\mu\text{L}/\text{min}$  with exposure of 120 ms; (c) PBS and R6G were perfused at the flow rates of 0.6  $\mu\text{L}/\text{min}$  0.2  $\mu\text{L}/\text{min}$

with exposure of 120 ms. (d) PBS and R6G were perfused at the flow rates of 0.6  $\mu\text{L}/\text{min}$  and 0.2  $\mu\text{L}/\text{min}$  with exposure of 200 ms. (e) Quantitative analysis of fluorescence intensity of R6G.

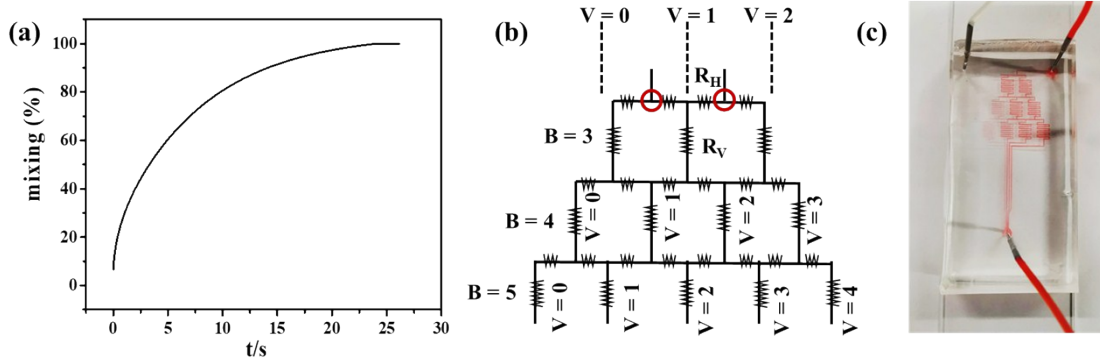


**Fig.S3** (a) The curve of percent mixing with time in the Christmas tree-shaped microfluidic chip. (b) Equivalent electronic circuit model of the fluid networks. (The red circles indicate the bifurcation point.) (c) The image of concentration gradient of red dye in microfluidic device.

Solutions containing RG6 and PBS were introduced from the top two inlets respectively. Each of them split at the bifurcation point and merged to mix along the serpentine microchannels. The distinct concentration gradient of the solution can be established on chip by repeating the process of splitting, combining and mixing in the network.<sup>2</sup> In order to ensure the intensive mixing, the length of the channels is determined by one-dimensional diffusion equation 1,

$$C(t, x) = \frac{1}{2} C_0 \sum_{n=-\infty}^{\infty} \left\{ \text{erf} \frac{h + 2nl - x}{2\sqrt{Dt}} + \text{erf} \frac{h - 2nl + x}{2\sqrt{Dt}} \right\} \quad (1)$$

where  $C_0$  is the initial concentration in the channel and  $C(t, x)$  is the concentration at a given time  $t$  at position  $x$ .  $D$  represents the diffusion coefficient;  $h$  and  $l$  are the height and width of the channel. According to the Eq1, we can obtain the mixing percentage at time  $t$  along the channel after substituting relevant size of channel from equation 2,

$$\% \text{mixing}(t) = \left( 1 - \frac{\int_0^l |C(t) - C(\infty)| dx}{\int_0^l |C(0) - C(\infty)| dx} \right) \times 100\% \quad (2)$$

where  $C(0)$ ,  $C(\infty)$  and  $C(t)$  are the concentration across the width of the channel at times  $t=0$ ,  $t=\infty$  and  $t$ . The result was shown in Fig.S3a and c, 97% mixing was obtained after 20 s, which satisfied the basic condition to generate the concentration.

The characteristics of the concentration generator can be known by analogy between the fluid behavior in the networks and the equivalent electronic circuit shown in Fig.S3b. Refer to the model of Noo Li Jeon et al<sup>1-2</sup>, the relative volume of the left and right solutions can be calculated accurately at the bifurcation point. The result that the same volume solution from left and right mix at each branch indicates the symmetric structure of this device. As shown in the Fig. 1d, the normalized concentration profiles demonstrated linear relationship with the number of outlets.

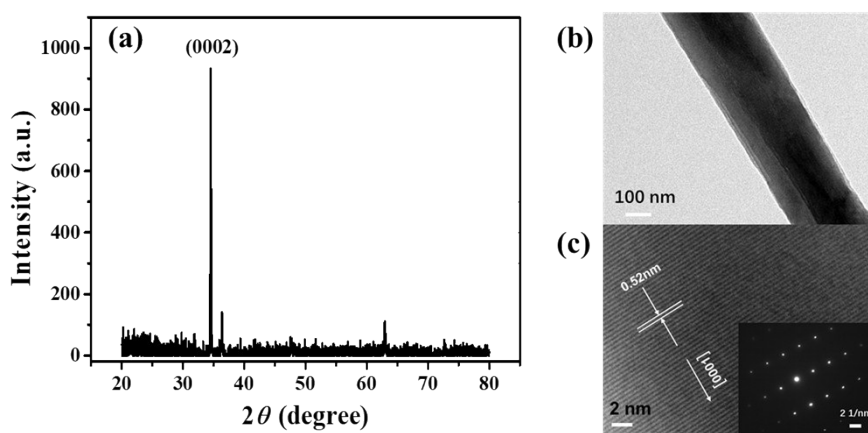


**Fig.S4** (a) XRD pattern of ZnO NRs. (b) TEM image; (c) HRTEM image and the corresponding selected-area electron diffraction (SAED) pattern (inset).

## References

- [1] Y. Wang, T. Mukherjee and Q. Lin, *J. Micromech. Microeng.*, 2006, 16, 2128-2137
- [2] N. L. Jeon, S. K. W. Dertinger, D. T. Chiu, I. S. Choi, A. D. Stroock and G. M. Whitesides, *Langmuir.*, 2000, 16, 8311-8316.